Dalton Transactions

RSC Publishing

PAPER

View Article Online
View Journal | View Issue

Cite this: *Dalton Trans.*, 2013, **42**, 12157

A modified cyclen azaxanthone ligand as a new fluorescent probe for Zn^{2+}†

Hela Nouri,[a,b] Cyril Cadiou,*[a] Latévi Max Lawson-Daku,[c] Andreas Hauser,[c] Sylviane Chevreux,[a] Isabelle Déchamps-Olivier,[a] Fabien Lachaud,[a] Riadh Ternane,[b] Malika Trabelsi-Ayadi,[b] Françoise Chuburu[a] and Gilles Lemercier*[a]

Received 9th May 2013,
Accepted 15th June 2013

DOI: 10.1039/c3dt51216a

www.rsc.org/dalton

A new cyclen derivative **L**, bearing a methyl-chromeno-pyridinylidene hydrazone moiety, was synthesized and studied in MeOH, as potential fluorescent "*OFF-on-ON*" sensors for Zn(II). Photophysical properties of this ligand being PET regulated, **L** was only weakly emissive in the absence of metal ions (OFF). **L** fluorescence was increased modestly upon addition of one equivalent of Zn(II), and further increased upon addition of a second equivalent. Therefore, Zn : **L** behaved as a highly sensitive ON sensor for zinc. This efficiency was correlated to Zn(II) coordination *via* the hydrazone moiety of the fluorophore, producing an efficient CHelation-Enhanced Fluorescence (CHEF) effect. A complementary theoretical study carried out with DFT calculations further elucidated the optical properties.

Introduction

The design of fluorescent probes for selective and sensitive quantification of important species, especially transition metal ions, has attracted considerable attention in analytical chemistry, especially for biochemistry and environmental chemistry.[1] The goal is to produce selective sensors able (i) to discriminate between a pool of metal ions the one to be specifically detected and (ii) to determine its concentration even at trace levels. From a biological point of view, Zn(II) is a frequently addressed target for sensing since it is widely present in living systems and influences a variety of processes. Zn(II) is involved in enzymatic activity, DNA synthesis, gene expression and apoptosis, as well as in some neurodegenerative disorders.[2] Among the methods developed for this purpose, fluorescence reveals itself as a powerful tool to sense this intrinsically spectroscopic silent ion, due to its simplicity and to its sensitivity.[3] The modulation of the emission by chelation of metal ions was first developed by L. R. Sousa and colleagues, using naphthalene derivatives.[4] Chemo-sensors constituting a binding unit (ionophore) covalently linked to a signalling unit (fluorophore) represent efficient and sensitive systems for the detection of these ions.[5] Binding of metal ions to the ionophore may affect the photophysical properties of the fluorophore giving rise to a specific optical response. One of the most applied fluorescence mechanisms, which allow signal transduction, is based on a CHelation-Enhanced Fluorescence (CHEF) effect.[6] This effect under Zn complexation was first highlighted on the fluorescence properties of anthracene derivatives.[7] There is therefore significant interest in developing effective fluorescent probes for which metal complexation is strong and controlled, from a stoichiometric point of view. For this purpose, tetraazamacrocycles,[8] and especially 1,4,7,10-tetraazacyclododecane (cyclen),[9] have often been the ionophores of choice, their other advantage being complexation selectivity, an important characteristic for selective sensing. Recently, some of us have proposed potential sensitive fluorescent chemosensors for which the binding unit is a cyclen moiety and the signalling unit a benzimidazole pendent group.[10] For these fluoroionophores, the Stokes shift was small which is far from being optimal for an effective detection, and their detection wavelength (around 300 nm) was not well-suited for analyses in a biological environment. In the present work, we report on a new mono-*N*-functionalised cyclen for which the gap between excitation and emission wavelengths was increased. In order to fulfill this aim, a fluorophore derived from an antenna used till now for lanthanide sensitizing (*i.e.* an azaxanthone moiety[10]) was grafted onto the macrocyclic cavity. This paper describes the coordination and the optical properties of the resulting cyclen methylchromeno-pyridinylidene hydrazone (**L**, Scheme 1) synthesized *via* the

[a]*Université Reims Champagne-Ardenne – Institut de Chimie Moléculaire de Reims, CNRS UMR n° 7312, Groupe Chimie de Coordination, UFR Sciences, BP 1039, 51687 Reims Cedex 2, France. E-mail: Cyril.cadiou@univ-reims.fr, gilles.lemercier@univ-reims.fr; Tel: +33 (0)3 26 91 32 40*
[b]*Laboratoire d'Application de la Chimie aux Ressources et Substances Naturelles et à l'Environnement – Université de Carthage, Faculté des Sciences de Bizerte, 7021 Bizerte, Tunisia*
[c]*Faculté des Sciences – Université de Genève, 30 quai Ernest Ansermet, CH-1211 Genève 4, Suisse, Switzerland*
†Electronic supplementary information (ESI) available. See DOI: 10.1039/c3dt51216a

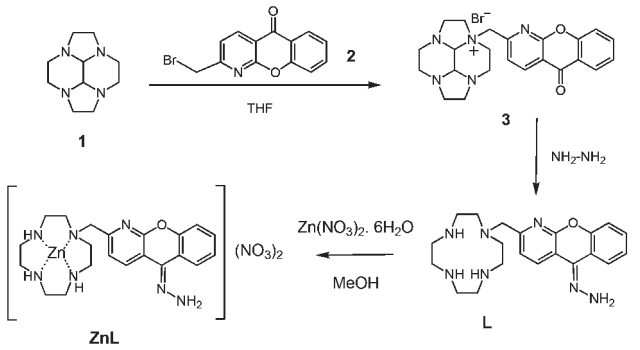

Scheme 1 Reagents and conditions for the synthesis of ligand **L** and its related zinc complex Zn : **L**.

two-step bis-aminal methodology.[12] Spectrophotometric and spectrofluorimetric investigations of the ligand in the presence of Zn(II) are reported to test whether **L** is a good candidate for the zinc detection. A theoretical study has also been performed in order to interpret the experimental data, especially to attribute the electronic transitions.

Results and discussion

Synthesis

The new ligand **L** was synthesized in three steps by condensation of glyoxal to cyclen followed by the alkylation of the resulting cyclen-glyoxal **1** in THF solution, with an equimolar amount of bromomethylazaxanthone **2** (2-(bromomethyl)-5*H*-chromeno[2,3-*b*]pyridin-5-one)[11] (Scheme 1). Hydrazinolysis of the intermediate monosalt **3** (in the presence of more than 50 equivalents) led to the deprotection of the macrocyclic moiety and to the simultaneous conversion of the ketone function into hydrazone.[13]

The intermediate **3** and the ligand **L** were characterized using ^{1}H, ^{13}C, IR spectroscopies, ESI-MS and CHN analysis (see the Experimental section). The cyclen-glyoxal alkylation was easily monitored by the evolution of the ^{13}C spectrum, especially in the macrocyclic ^{13}C area (between 40 and 60 ppm). Since the alkylation of the macrocycle decreased its symmetry, an increase of the number of ^{13}C peaks was observed on going from compound **1** (two signals at 50.2 and 51.3 ppm) to compound **3** (at least seven signals between 43.4 and 62.7 ppm). Concomitantly, the aminal carbons of **1** (77.7 ppm) were no longer equivalent and the mono-*N*-alkylation of **1** rendered these carbon anisochronous (72.1 and 84.4 ppm in **3**). For the aromatic part of the spectrum, the ^{13}C carbonyl signal of the azaxanthone moiety was observed at 179.8 ppm. Further deprotection of **3** into **L** was accompanied by recovery of a local symmetry for the macrocyclic subunit (observed as four distinct peaks for the macrocyclic carbon atoms between 44 and 53 ppm) and by the disappearance of the ^{13}C signals corresponding to the bis-aminal bridge. At least for the azaxanthone part of the spectrum, the disappearance of the ^{13}C carbonyl signal (δ = 178.9 ppm) to the benefit of a ^{13}C hydrazone-type signal at 161.9 ppm could be ascribed to the hydrazone exocyclic function in **L**. This structural modification was further confirmed by ESI-HRMS analysis and IR analysis with the disappearance of the carbonyl elongation vibration (1658 cm^{-1} in **3**) in favour of a C=N vibration in **L** (1589 cm^{-1}).

In order to obtain the Zn : **L** complex, one equivalent of **L** was reacted with a slight excess of $Zn(NO_3)_2$ in a methanol solution (procedure described in the Experimental section). The complex was isolated after precipitation with the addition of diethyl ether. The comparison of the ^{1}H NMR spectra of **L** and $[Zn : \mathbf{L}](NO_3)_2$ underlined modifications in the chemical shifts upon coordination of the ligand to the zinc ion. Actually, four signals at 7.00, 7.32, 7.97 and 8.60 ppm in CD_3OD were attributed to the **L** aromatic protons. Upon complexation, these signals are shifted to 7.06, 7.34, 7.82, and 8.80 ppm, respectively. The same observation can be made for the CH_2 geminal protons borne by the methylene group in the α position of the macrocycle (upfield shift from 3.94 ppm in **L** to 4.37 ppm in $[Zn : \mathbf{L}](NO_3)_2$).

Photophysical properties

Electronic absorption spectroscopy. Absorption spectra in MeOH of **L** alone and in the presence of increasing amounts

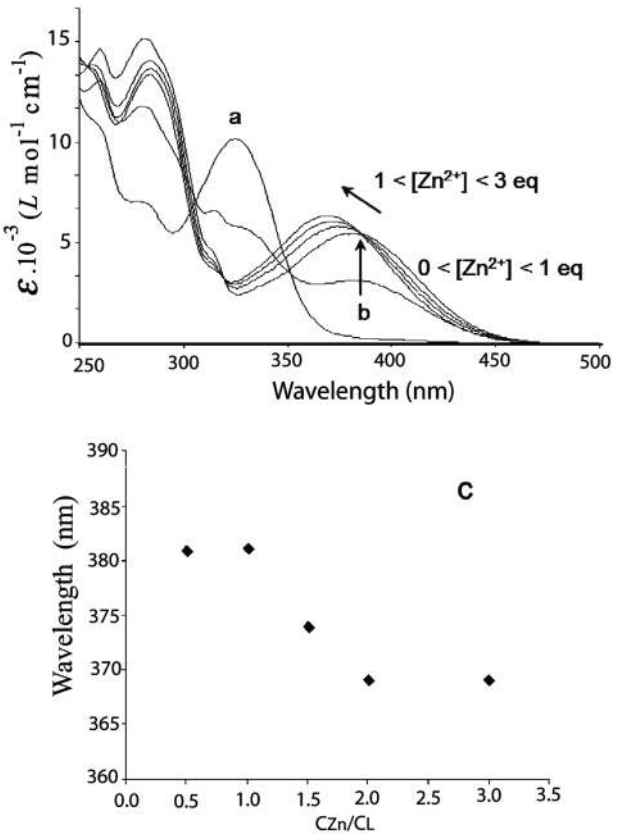

Fig. 1 (a) Absorption spectra of **L** in MeOH ([**L**] = 1.2 × 10^{-5} mol L^{-1}) and (b) in the presence of various concentrations of Zn^{2+} (0.5, 1, 1.5, 2 and 3 equiv. to the probe concentration); (c) evolution of the position of the lowest energy absorption maximum as a function of Zn^{2+} addition.

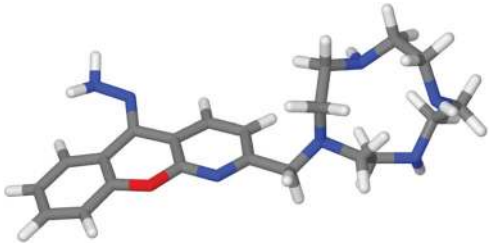

Fig. 2 Optimized geometry of **L** in MeOH (PBE-D3/TZP results).

of Zn^{2+} are reported in Fig. 1. In MeOH, the longest wavelength band of **L** is centred at 325 nm (ε = 10 000 L mol^{-1} cm^{-1}, Fig. 1a). This band position does not deviate significantly from those reported for azaxanthone in EtOH (329 nm, ε = 6640 L mol^{-1} cm^{-1})[13] or 2-methyl-1-azaxanthone[11] (330 nm, ε = 6900 L mol^{-1} cm^{-1}).

According to the solvent polarity, this band exhibits a slight blue shift from 331 nm (diethyl ether) to 324 nm (DMSO). This is in accordance with an n → π* character[14] for the longer wavelength absorption of the chromophore methylchromenopyridinylidene hydrazone. However, since the amplitude of the shift is rather small, one cannot exclude the contribution and/or mixing of these transitions with π → π* transitions.

In order to understand the absorption properties of **L**, its structure in MeOH has been optimized using Density Functional Theory (DFT)[15] and its lowest-lying excited states[16] have been characterized by time-dependent DFT (TDDFT) calculations. The optimized geometry of **L** is shown in Fig. 2.[17]

The free ligand **L** is predicted to adopt an open conformation. The energies and oscillator strengths of the $S_0 \rightarrow S_n$ electronic transitions (n = 1,...,30) calculated for **L** are summarized in Table S1 of the ESI,† along with the major molecular orbital (MO) → MO contributions. Some of the frontier MOs involved in these transitions are presented in Fig. 3. The lowest-energy electronic transition $S_0 \rightarrow S_1$ is a HOMO → LUMO transition (99%, see Table S1 in ESI†), and it is thus an n → π* charge-transfer (CT) transition from the cyclen to the azaxanthone-hydrazone moiety. This is in good agreement with the photo-induced electron transfer (PET) mechanism, between the macrocyclic amine functions and the fluorophore, before the complexation of the zinc ion.

The characterized $S_0 \rightarrow S_n$ (n = 1,...,30) transitions span the 17 600–40 200 cm^{-1} (*i.e.*, 245–570 nm) energy range and consist of mostly n → π* charge-transfer (CT) transitions of weak to vanishing intensities. The transitions of high intensities are π–π* transitions centred on the azaxanthone-hydrazone fragment. For example, this is the case of the $S_0 \rightarrow S_7$ transition located at 26 090 cm^{-1} (*i.e.* 3.235 eV = 383 nm), which primarily involves the HOMO − 3 → LUMO transition (75%, see Fig. 6), and has an oscillator strength of 0.1120.

Upon Zn^{2+} complexation (Fig. 1b), the absorption spectra shift towards longer wavelengths, in a concentration-dependent manner. The longest wavelength band appeared at 380 nm (ε = 5300 L mol^{-1} cm^{-1}) upon addition of one equivalent of Zn^{2+} and undergoes a blue shift to 370 nm upon addition of a second equivalent of Zn^{2+} (Fig. 1c). This evolution could account for the successive formation of 1 : 1 and 2 : 1 (metal : **L** ratio) Zn^{2+} complexes. Along this line, the isosbestic points observed at ~310 nm and ~350 nm, and at ~320 nm and ~385 nm from zero to one equivalent Zn^{2+}, and from one to two, respectively, can be associated with the coexistence in different ratios of **L** and the 1 : 1, and 2 : 1 complexes in solution (Fig. 1). The results of the TDDFT excitation calculations performed on the optimized geometry are summarized in the ESI.† They show that the lowest energy absorption band of Zn : **L** is due to two intense π–π* electronic transitions centred on the azaxanthone-hydrazone moiety (Table S3†). Namely, (1) the lowest-energy $S_0 \rightarrow S_1$ electronic transition found at 22 904 cm^{-1} (*i.e.*, 2.840 eV ≈ 437 nm) with an oscillator strength of 0.0604, which is mainly a HOMO → LUMO transition (83%), and (2) the $S_0 \rightarrow S_3$ electronic transition located at 27 441 cm^{-1} (*i.e.*, 3.402 eV ≈ 364 nm) with an oscillator strength of 0.0309, which is mainly a HOMO → LUMO + 1 transition (62%). The frontier orbitals of Zn : **L** involved in electronic transitions are presented in Fig. 4.

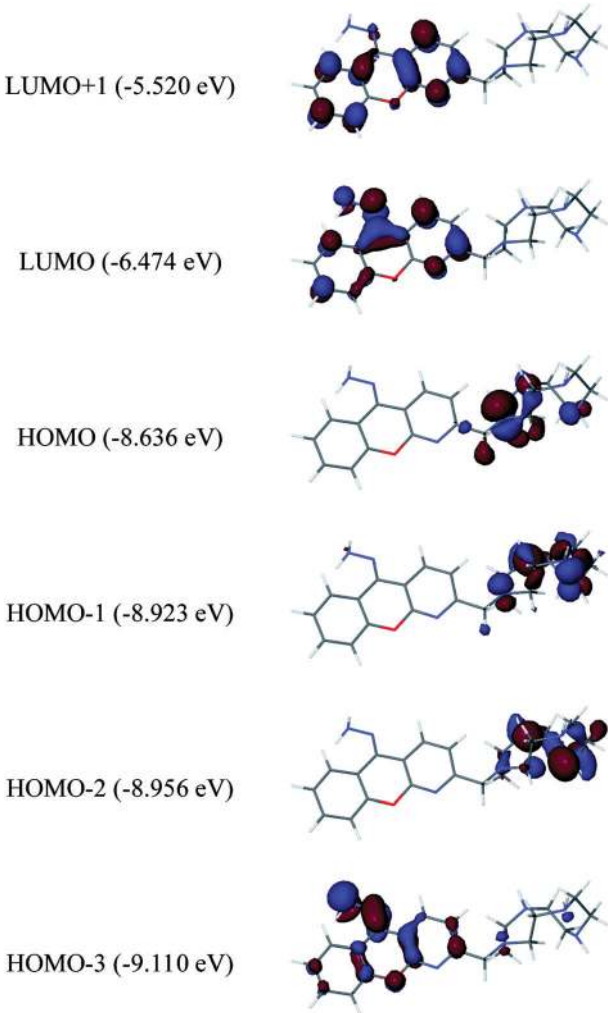

Fig. 3 Frontier molecular orbitals of **L** in MeOH (SAOP/TZP results).

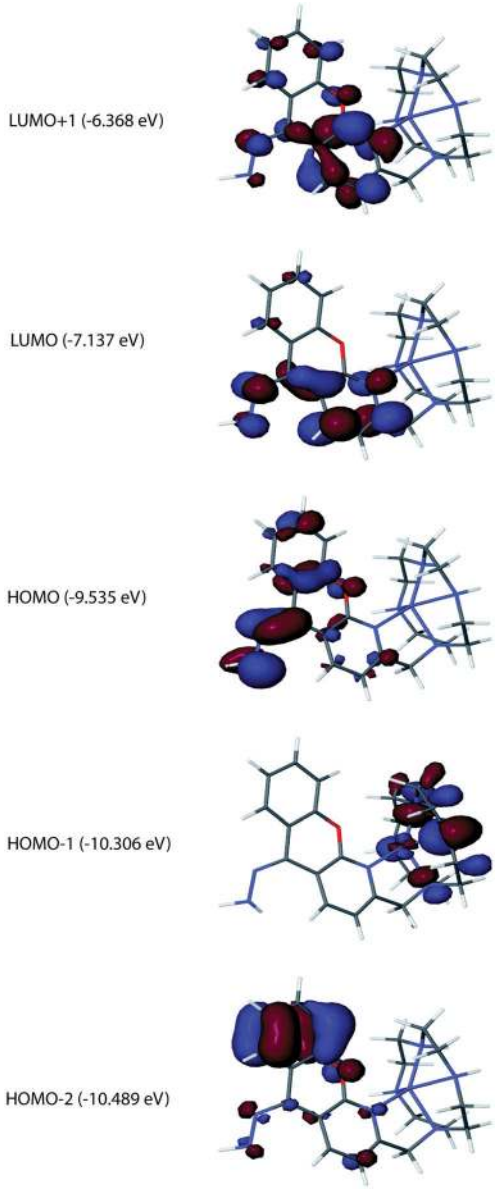

Fig. 4 Frontier molecular orbitals of Zn : **L** in MeOH (SAOP/TZP results).

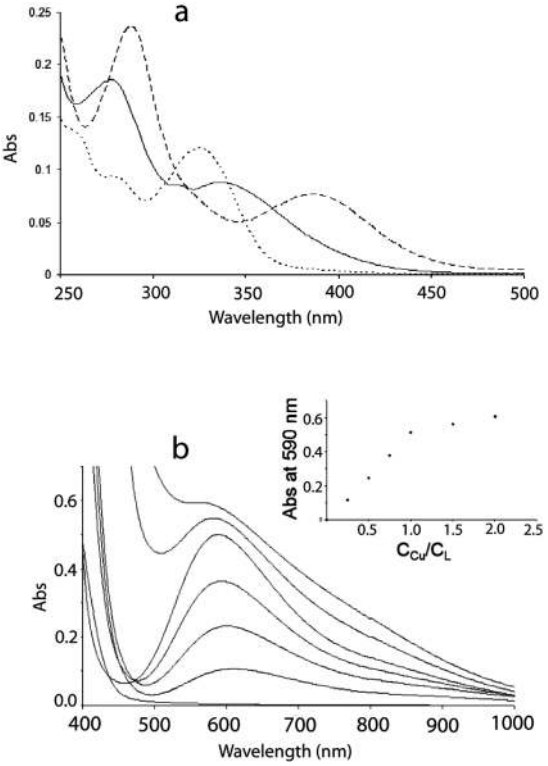

Fig. 5 (a) Evolution of the UV absorption spectrum of a 1.25×10^{-5} mol L^{-1} solution of **L** (dotted lines) upon Cu^{2+} addition in MeOH (1 equiv. plain lines, 2 equiv. dashed lines). (b) Evolution of the visible absorption spectrum of a 2×10^{-3} mol L^{-1} solution of **L** upon Cu^{2+} addition in MeOH (0, 0.25, 0.5, 0.75, 1, 1.5 and 2 equiv. to the probe concentration). Inset: evolution of the intensity of the 590 nm absorption of **L** as a function of Cu^{2+} addition.

The TDDFT results indicate that the low energy absorption band of Zn : **L** also includes the $S_0 \rightarrow S_2$ and $S_0 \rightarrow S_4$ electronic transitions of weak intensities located at 25 629 cm^{-1} (*i.e.*, 3.177 eV ≈ 390 nm) and 27 846 cm^{-1} (*i.e.*, 3.452 eV ≈ 358 nm), respectively. The former involves the HOMO − 1 → LUMO transition (100%) and (Fig. 4) is thus attributed to an n–π* charge-transfer transition from the cyclen to the azaxanthone-hydrazone moiety; the latter is mainly a HOMO − 2 → LUMO transition (78%) and remains a π–π* electronic transition centered on the azaxanthone-hydrazone moiety.

Upon addition of Cu^{2+} to a solution of **L**, the same conclusions can be drawn on the basis of the evolution of the longest wavelength absorption band for **L** (325 nm, see Fig. 5a). The addition of the first equivalent of Cu^{2+} is accompanied by a shift to 335 nm, and the addition of the second equivalent induces a more pronounced red shift of this band to 390 nm.

Furthermore, in the visible region, an absorption band is observed at 610 nm (ε = 130 L mol^{-1} cm^{-1}) and its intensity increases linearly with the amount of copper until a 1 : 1 stoichiometry is reached (Fig. 5b). This absorption may be attributed to a d → d* transition of the macrocyclic copper complex, the ε value being typical for a square-pyramidal complex with a pentacoordinated copper(II) cation.[18]

Such a pentacoordination of the transition metal ion is supported by the optimization results obtained for the $[Zn : L]^{2+}$ complex. The ligand indeed adopts upon metallation a closed conformation, which allows for the pentacoordination of Zn^{2+} (Fig. 6).

Regarding the complexation of the second equivalent of the metal, the absorption spectrum of **L** with adjunction of copper gives additional insight into this process. No further absorbance evolution is observed for the transition at 610 nm when subsequent copper addition is performed (from 1 to 2 equivalents, see Fig. 5). This supports the hypothesis that the first formed complex (1 : 1 complex) corresponds to the insertion of the first equivalent of metal in the macrocyclic cavity, the second equivalent of metal being probably coordinated by the hydrazone function (see Scheme 2).

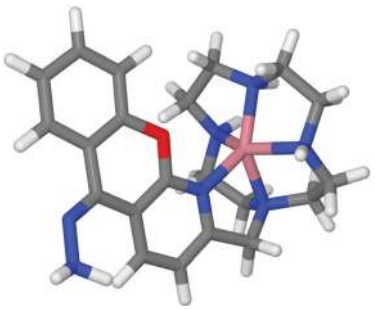

Fig. 6 Optimized geometry of Zn : **L** in MeOH: the Zn^{2+} ion exhibits a distorted square pyramidal coordination, with a basal plane defined by the average plane of the four N atoms of the cyclen fragments. The optimized basal Zn–N bond lengths range from 2.070 Å to 2.176 Å, and the optimized apical Zn–N bond length is 2.048 Å.

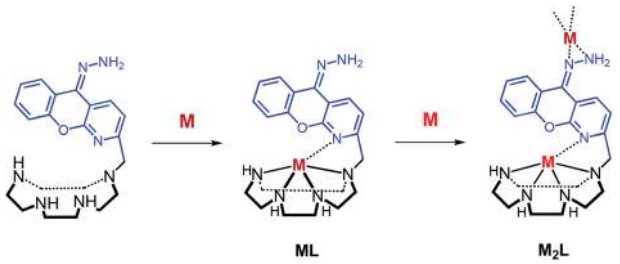

Scheme 2 Probable complexation mechanism of two equivalents of M^{2+} (Zn^{2+}, Cu^{2+}) by **L**.

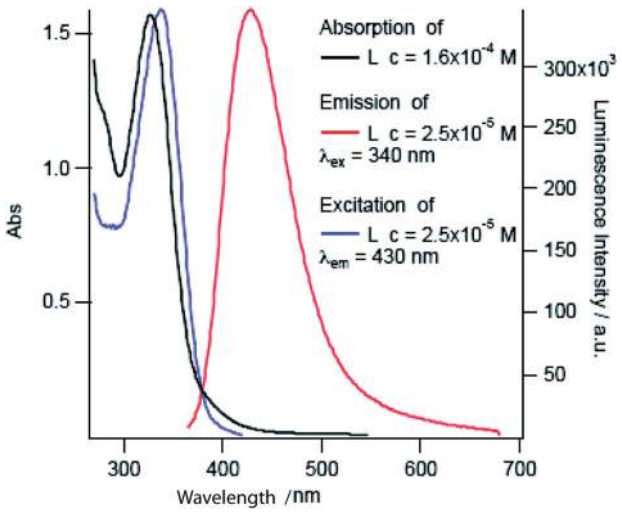

Fig. 7 Absorption, excitation, and emission spectra of **L** in MeOH.

Spectrofluorimetric study of L in MeOH. The luminescent response of **L** was investigated in MeOH ($c = 2.5 \times 10^{-5}$ mol L^{-1} at 25 °C). The absorption, excitation, and emission spectra are reported in Fig. 7.[19]

Excitation at 320 nm gave an emission spectrum maximum at 430 nm. The Stokes shift is of 7990 cm^{-1} and it becomes even larger (around 9920 cm^{-1}) in the solid state (see Fig. S1 in the ESI†). In MeOH, **L** is poorly fluorescent ($\phi \approx 0.4\%$).

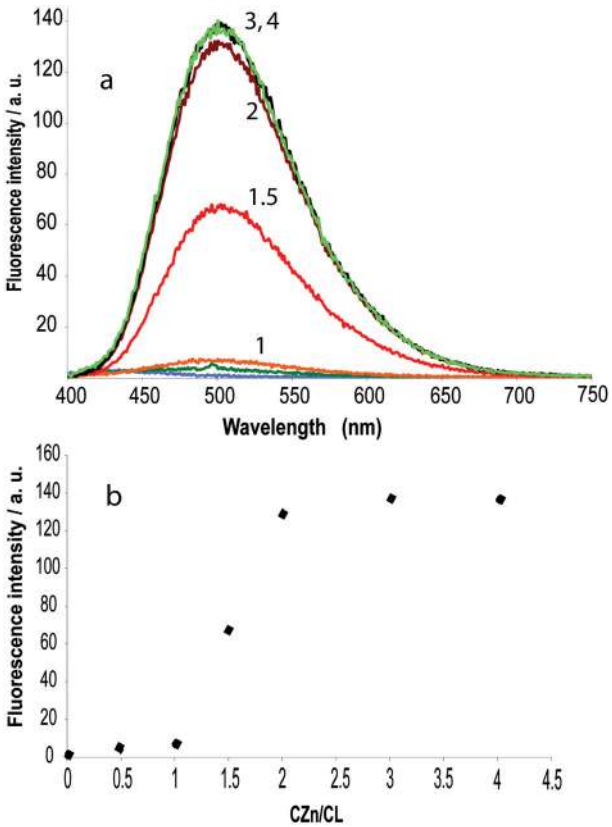

Fig. 8 (a) Evolution of the emission spectrum of a 1.2×10^{-5} mol L^{-1} solution of **L** upon Zn^{2+} addition in MeOH (0, 0.5, 1, 1.5, 2, 3 and 4 equiv. to the probe concentration). (b) Evolution of the intensity of the 505 nm emission as a function of Zn^{2+} addition (λ_{exc} = 360 nm).

In the presence of increasing amounts of Zn^{2+}, the fluorescence increases (Fig. 8).

The relative emission of **L** increased linearly by a factor of 8 with one equivalent of Zn^{2+} and then by a factor of about 20 with the addition of a second equivalent of Zn^{2+}. This implied that the increase in fluorescence was stoichiometric and was probably due to the formation of the 1 : 1 and 2 : 1 Zn : L complexes, as previously deduced from UV measurements.

This behaviour could be attributed to the blocking of a photo-induced electron transfer (PET) between the ligand amine functions (from macrocyclic and hydrazone moieties) and the fluorophore.[6,10,13]

The results of the TDDFT calculations performed on the optimized ground-state geometry of **L** gave the T_1 state at 17 317 cm^{-1} (*i.e.*, 2.147 eV ≈ 577 nm) above the S_0 ground state, with the $S_0 \rightarrow T_1$ transition involving mainly the HOMO → LUMO transition (98%) and thus being an $n \rightarrow \pi^*$ charge-transfer (CT) transition from the cyclen to the azaxanthone-hydrazone fragment. The presence of the $S_0 \rightarrow T_1$ transition at about 580 nm corroborates the possible partial triplet character of the emissive lowest-energy excited state of the ligand, so that this one may be of interest in lanthanide sensitisation.[11] The efficiency of the $(\pi \rightarrow \pi^*)^1 \rightarrow (n \rightarrow \pi^*)^3$ intersystem crossing has already been well commented in the literature [El Sayed

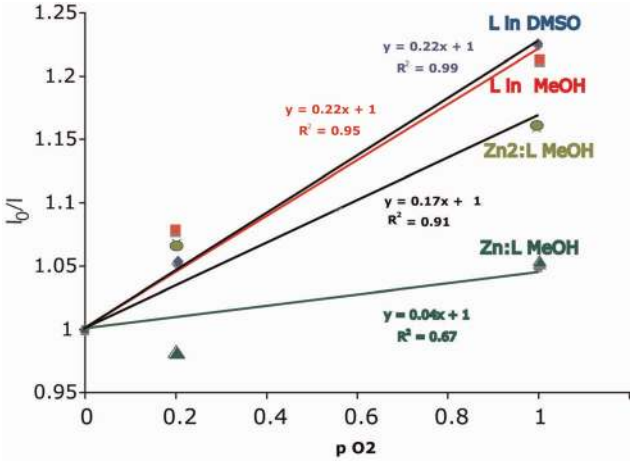

Fig. 9 Dependence of the I_0/I value on the oxygen partial pressure for ligand **L** in MeOH (square) and in DMSO (rhombus), after addition of one equivalent of Zn^{2+} and two equivalents of Zn^{2+}.

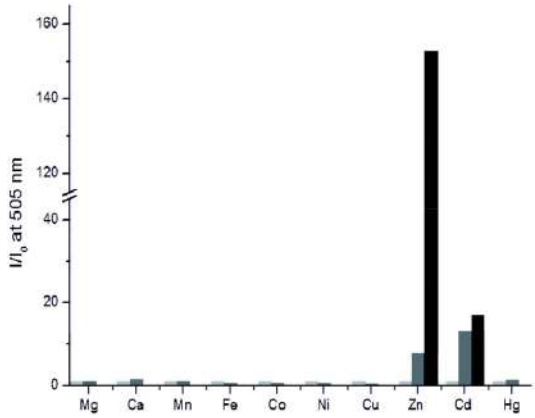

Fig. 10 Relative fluorescence of **L** (light grey bars) in MeOH at 505 nm responding to 1 equivalent (grey bars) and 2 equivalents (dark grey bars) of the metal ions ([**L**] = 1.2×10^{-5} mol L^{-1}, T = 25 °C, λ_{exc} = 360 nm). I_0 is the emission intensity of **L** at 505 nm in the absence of metal ions.

rules], and in our case TDDFT calculations show many n → π* triplet states available (data reported in ESI†). The possible triplet character of the emissive state of lowest energy is also consistent with the relative efficiency of the energy transfer between the excited **L** and the fundamental triplet oxygen as shown in Fig. 9. Actually, in fluid solution, the dependence of emission intensity and lifetime on quencher concentration is given by the following Stern–Volmer equations (eqn (1)):

$$\frac{I_0}{I} = 1 + K_{SV}[O_2] = 1 + k_q t_0[O_2] \quad (1)$$

where the I_s parameters are emission intensities, the τ_s are lifetimes, K_{SV} is the Stern–Volmer quenching constant, and k_q is the bimolecular rate constant for quenching of the excited state. The subscript 0 denotes the values of the quantity in the absence of the quencher. Plots of I_0/I *versus* oxygen concentration will be linear with identical slopes equal to K_{SV} if there is a single class of luminophores that are all equally accessible to the quencher. That is what was observed in this case for ligand **L**, either in MeOH or in DMSO (the solvent for which the emission signal is higher; a detailed study is under way). The slope was determined and is equal to 0.22. This higher value for the free **L** ligand, as compared to the one of 0.04 found for the Zn : **L** complex, may suggest a less efficient quenching with triplet dioxygen from the emissive state for this last one. This point is also in agreement with a more pronounced luminescence in non-deoxygenated solution for Zn : **L**, with the same quantum yield (0.3%, and 0.4% for Zn : **L**, and **L**, respectively; see ESI† for the measurements).

Quantum yield for the Zn_2 : **L** complex is actually around 6.5 times greater (2.6%), which can partially explain the large increase in luminescence properties. The factor of 20 observed in the titration experiment is also due to the increase in extinction coefficient at the excitation wavelength of 360 nm upon addition of Zn^{2+} (see Fig. 5a).

Finally, an important feature of a potential fluorescent Zn^{2+} sensor is its ability to sense selectively this ion over other endogenous relevant cations. To determine whether **L** worked as a selective chemosensor for Zn^{2+}, the fluorescence response of **L** was recorded in MeOH, in the presence of a series of divalent cations (some first-row transition metals, Cd^{2+}, Hg^{2+} and relevant alkaline earth ions, see Fig. 10).

L fluorescent intensities did not evolve by addition of ions that are found in high concentrations in cells, such as Mg^{2+} and Ca^{2+}. This result was as expected because cyclen is not a good receptor for alkaline earth cations, whence its absence of response in the presence of these ions. Addition of metals such as Mn^{2+}, Fe^{2+}, Co^{2+} and Ni^{2+} did not modify **L** fluorescence while addition of Cu^{2+} induced an expected fluorescence decrease.[10,20] The greatest advantage of **L** was its exceptional response to zinc. The test showed again that even if the addition of the first equivalent of Zn^{2+} was accompanied by a modest exaltation of the fluorescence, the addition of the second equivalent gave rise to great signal exaltation.

Similar behaviour was obtained for Cd^{2+}, although the enhancement was widely poorer. This noteworthy difference could be used to distinguish favourably between Zn^{2+} and Cd^{2+}.

Conclusions

This paper has described the synthesis and the coordination behaviour towards Zn^{2+} of a new fluorescent cyclen sensor **L**. In MeOH, the photochemical properties of this ligand were PET regulated and **L** was non-emissive in the absence of metal ions (OFF). The presence of Zn^{2+} triggered the fluorescence of **L** in two phases (on-ON). At first, the addition of a first equivalent induced a modest optical response (on). Subsequently, the addition of the second equivalent was accompanied by a significant signal enhancement (ON). The coordination mechanism of **L** allowed us to propose that the first modest CHEF effect corresponded to the complexation of one Zn^{2+} ion into

the macrocyclic cavity, while the second and important CHEF effect could be associated with a second Zn^{2+} chelation by the hydrazone moiety. Finally, the selectivity test has shown that the fluorescence response of **L** is highly specific towards Zn^{2+}, which makes this new ligand an efficient and selective probe for this ion. Further experiments are in progress to increase the solubility of this ligand in aqueous media for potential biological applications. Studies are in progress to deepen our knowledge of this edifice (especially the dependence on the nature of the solvent), and potential applications of its interesting emission properties at the solid state.

Experimental section

Calculations

All calculations have been performed with the ADF program package,[16] using, for the geometry optimizations, the PBE functional,[21] augmented with the semi-empirical long-range dispersion correction from Grimme (PBE-D3),[22] and for the TDDFT calculations, the SAOP exchange-correlation potential.[23] Solvent effects were taken into account using the Conductor like Screening Model (COSMO) of solvation[24] as implemented in ADF.[25] The atoms were described in all calculations by the TZP basis set of triple-ξ polarized quality from the ADF Slater-type orbital (STO) basis set database;[26] in the optimization calculations, the core levels were kept frozen up to the 1s level for the N, C, and O atoms and up to the 2p level for the Zn atom.

Synthesis

Procedure for cyclen-glyoxal-azaxanthone 3. In a flask equipped with a magnetic stirring system containing 7 mL of anhydrous THF, 61 mg (0.314 mmol) of cyclen-glyoxal **1** were added dropwise to 8 mL of a solution of 2-bromomethyl-1-azaxanthone **2** (100 mg, 0.345 mmol) in THF. The solution was stirred at room temperature under an inert atmosphere for 20 hours, allowing the formation of a pale precipitate, which corresponded to the mono-*N*-functionalized compound **3** (145 mg, 96% yield). ^{1}H NMR for **3** (250.13 MHz, D_2O, ppm) δ 2.5–4.1 (m, 16H, NCH_2), 4.19 (s, 1H, NC*H*N), 4.50 (m, 1H, NC*H*N), 4.98 (d, J = 12.5 Hz, 1H, NC$H_{2\text{-}Ar}$), 5.20 (d, J = 12.5 Hz, 1H, NC$H_{2\text{-}Ar}$), 7.55 (t, J = 7.5 Hz, 1H, H_{Ar}), 7.67 (d, J = 10 Hz, 1H, H_{Ar}), 7.78 (d, J = 10 Hz, 1H, H_{Ar}), 7.95 (t, J = 7.5 Hz, 1H, H_{Ar}), 8.22 (d, J = 7.5 Hz, 1H, H_{Ar}), 8.80 (d, J = 7.5 Hz, 1H, H_{Ar}). ^{13}C NMR for **3** (62.9 MHz, D_2O, ppm) δ 44.3, 48.1, 48.5, 48.7, 51.8, 59.0, 63.6 (*C*H_2N), 72.1, 84.4 (C_{am}); 117.4, 118.8, 121.0, 124.4, 126.0, 126.6, 137.7, 140.1, 153.8, 156.0, 160.0 (C_{Ar}), 179.8 (C=O). MS m/z (TOF MS ES$^+$) calculated for $C_{23}H_{26}N_5O_2^+$ [M^+], 404.2; found 404.2. Anal. found (%) C, 57.69; H, 5.81; N, 13.46; $C_{23}H_{26}BrN_5O_2$. 0.5 THF requires (%) C, 57.46; H, 6.01; N, 13.43. IR (KBr): $\nu_{(C=O)}$: 1658 cm^{-1}.

Deprotection. Functionalized cyclen-glyoxal-azaxanthone **3** (263 mg, 0.543 mmol) is deprotected using hydrazine monohydrate (5.3 mL, 109.3 mmol). The reaction mixture was stirred for 4.5 hours at 100 °C, and then at room temperature for 22 hours. After cooling, the deprotected compound **L** precipitates. The ligand is isolated by filtration and washed with water until having a white residue (80% yield) ^{1}H NMR (250.13 MHz, CD_3OD, ppm) δ 2.55–2.95 (m, 16H, NCH_2), 3.94 (s, 2H, NC$H_{2\text{-}Ar}$), 7.00 (m, 2H, H_{Ar}), 7.32 (m, 2H, H_{Ar}), 7.97 (d, J = 7.5 Hz, 1H, H_{Ar}), 8.60 (d, J = 7.5 Hz, 1H, H_{Ar}). ^{13}C NMR (62.9 MHz, CD_3OD, ppm) δ 45.5, 46.2, 47.1, 52.8 (*C*H_2N), 60.7 (Ar*C*H_2N), 113.2, 117.9, 118.0, 118.9, 120.7, 128.9, 130.5, 130.8, 133.7, 144.6, 157.4 (C_{Ar}), 161.9 (C=N). HRMS m/z (TOF MS ES$^+$) calculated for $C_{21}H_{30}N_7O^+$ [M + H^+]: 396.2512; found 396.2514. Anal. found (%) C, 62.13; H, 7.19; N, 23.91; $C_{21}H_{29}N_7O$. 0.5 H_2O requires (%): C, 62.35; H, 7.48; N, 24.24. IR (KBr): $\nu_{(C=N)}$: 1589 cm^{-1}.

Zn : L(NO$_3$)$_2$. A methanolic solution (5 mL) containing 39 mg of $Zn(NO_3)_2{\cdot}6H_2O$ (0.131 mmol) was added dropwise to 50 mg (0.126 mmol) of L dissolved in methanol (10 mL). The solution was refluxed for 5 hours and concentrated to a minimum by evaporation. A pale yellow powder was precipitated by addition of diethyl ether, and Zn : $L(NO_3)_2$ was collected by filtration (85% yield). ^{1}H NMR (250.13 MHz, CD_3OD, ppm) δ 2.70 < d < 3.27 (m, 16H, CH_2N), 4.37 (s, 2H, ArCH_2N), 7.06 (m, 2H, H_{Ar}), 7.34 (m, 2H, H_{Ar}), 7.82 (d, J = 7.5 Hz, 1H, H_{Ar}), 8.80 (d, J = 7.5 Hz, 1H, H_{Ar}). ^{13}C NMR (62.9 MHz, CD_3OD, ppm) δ 45.0, 46.3, 46.9, 54.0 (CH_2N), 59.0 (ArCH_2N), 117.6, 119.8, 121.2, 122.1, 126.9, 127.5, 130.2, 131.9, 137.6, 138.7, 142.3 (C_{Ar}), 156.7 (C=N). MS m/z (TOF MS ES$^+$) calculated for $C_{21}H_{28}N_7OZn^+$ [Zn : LH_{-1}]$^+$, 458.2; found 458.2; calculated for $C_{21}H_{29}N_7OZn^{2+}$ [Zn : **L**]$^{2+}$, 229.6; found 229.6. Anal. found (%) C, 40.10; H, 4.86; N, 19.88; $C_{21}H_{29}N_9O_7Zn$. 2.5 H_2O requires (%): C, 40.04; H, 5.44; N, 20.01. IR (KBr): $\nu_{(C=N)}$: 1607 cm^{-1}, $\nu_{(NO_3^-)}$: 1314 cm^{-1}.

Acknowledgements

Hela Nouri thanks the Tunisian Ministry of Higher Education and Scientific Research for her doctoral fellowship. Financial support from CNRS, Conseil Regional Champagne Ardenne, Conseil General de la Marne, Ministry of Higher Education and Research (MESR) and EU-programme FEDER to the PlAneT CPER project is gratefully acknowledged. G. L. thanks Elizabeth Boreham and Lucy Jones for linguistic advice during their training period in the Laboratory.

Notes and references

1 R. Ling, M. Yoshida and P. S. Mariano, *J. Org. Chem.*, 1996, **61**, 4439.
2 E. L. Que, D. W. Domaille and C. J. Chang, *Chem. Rev.*, 2008, **108**, 1517; H. Kozlowski, A. Janicka-Klos, J. Brasun, E. Gaggelli, D. Valensin and G. Valensin, *Coord. Chem. Rev.*, 2009, **253**, 2665.
3 A. W. Czarnik, *Fluorescent Chemosensors for Ion and Molecule Detection*, American Chemical Society, Washington, DC, 1993; E. Kimura and S. Aoki, *BioMetals*, 2001, **14**, 191;

E. M. Nolan and S. J. Lippard, *Acc. Chem. Res.*, 2009, **42**, 193, and references therein.

4 L. R. Sousa and J. M. Larson, *J. Am. Chem. Soc.*, 1977, **99**, 307.

5 L. Fabbrizzi and A. Poggi, *Chem. Soc. Rev.*, 1995, **24**, 197; A. W. Czarnik, *Acc. Chem. Res.*, 1994, **27**, 302.

6 A. P. De Silva, H. Q. N. Gunaratne, T. Gunnlaugsson, A. J. Huxley, C. P. Mc Coy, J. T. Rademacher and T. E. Rice, *Chem. Rev.*, 1997, **97**, 1515.

7 M. E. Huston, K. W. Haider and A. W. Czarnik, *J. Am. Chem. Soc.*, 1988, **110**, 4460.

8 E. U. Akkaya, M. E. Huston and A. W. Czarnik, *J. Am. Chem. Soc.*, 1990, **112**, 3590; S. Aoki, S. Kaido, H. Fujioka and E. Kimura, *Inorg. Chem.*, 2003, **42**, 1023; S. Aoki, K. Sakurama, N. Matsuo, Y. Yamada, R. Takasawa, S. Tanuma, M. Shiro, K. Takeda and E. Kimura, *Chem.–Eur. J.*, 2006, **12**, 9066; S. Aoki, K. Sakurama, R. Ohshima, N. Matsuo, Y. Yamada, R. Takasawa, S. Tanuma, K. Takeda and E. Kimura, *Inorg. Chem.*, 2008, **47**, 2747; E. Tamanini, A. Katewa, L. M. Sedger, M. H. Todd and M. J. Watkinson, *Inorg. Chem.*, 2009, **48**, 319; E. Tamanini, K. Flavin, M. Motevalli, S. Piperno, L. A. Gheber, M. H. Todd and M. Watkinson, *Inorg. Chem.*, 2010, **49**, 3789.

9 T. Koike, T. Watanabe, S. Aoki, E. Kimura and M. Shiro, *J. Am. Chem. Soc.*, 1996, **118**, 12696; R. Ohshima, M. Kitamura, A. Morita, M. Shiro, Y. Yamada, M. Ikekita, E. Kimura and S. Aoki, *Inorg. Chem.*, 2010, **49**, 888.

10 A. El Majzoub, C. Cadiou, I. Déchamps-Olivier, F. Chuburu and M. Aplincourt, *Eur. J. Inorg. Chem.*, 2007, 5087; A. El Majzoub, C. Cadiou, I. Déchamps-Olivier, F. Chuburu, M. Aplincourt and B. Tinant, *Inorg. Chim. Acta*, 2009, **362**, 1169.

11 P. Atkinson, K. S. Findlay, F. Kielar, R. Pal, D. Parker, R. A. Poole, H. Puschmann, S. L. Richardson, P. A. Stenson, A. L. Thompson and J. Yu, *Org. Biomol. Chem.*, 2006, **4**, 1707.

12 M. Le Baccon, F. Chuburu, L. Toupet, H. Handel, M. Soibinet, I. Déchamps-Olivier, J. P. Barbier and M. Aplincourt, *New J. Chem.*, 2001, **25**, 1168.

13 Y. Zhou, H. N. Kim and J. Yoon, *Bioorg. Med. Chem. Lett.*, 2010, **20**, 125.

14 J. Michl, *Handbook of Photochemistry*. Taylor & Francis Group, LLC, 6000 Broken Sound Parkway NW, 3rd edn, 2006, p. 19.

15 P. Hohenberg and W. Kohn, *Phys. Rev.*, 1964, **136**, B864; W. Kohn and L. J. Sham, *Phys. Rev.*, 1965, **140**, A1133.

16 The geometries of **L** and Zn : **L** were first optimized in the gas phase and the subsequent frequency analysis gave the calculated structures as true minima. These optimized gas-phase geometries were then used as starting points for the geometry optimizations performed in MeOH. The inclusion of the solvent effects proved to have little influence because the condensed-phase and gas-phase geometries of **L** and Zn : **L** are in both cases very similar (see Fig. S2 of the ESI†).

17 C. Fonseca Guerra, J. Snijders, G. te Velde and E. J. Baerends, *Theor. Chem. Acc.*, 1998, **99**, 391; G. te Velde, F. M. Bickelhaupt, E. J. Baerends, C. Fonseca Guerra, S. J. A. van Gisbergen, J. G. Snijders and T. Ziegler, *J. Comput. Chem.*, 2001, **22**, 931; E. J. Baerends, T. Ziegler, J. Autschbach, D. Bashford, A. Bérces, F. M. Bickelhaupt, C. Bo, P. M. Boerrigter, L. Cavallo, D. P. Chong, L. Deng, R. M. Dickson, D. E. Ellis, M. van Faassen, L. Fan, T. H. Fischer, C. F. Guerra, A. Ghysels, A. Giammona, S. J. A. van Gisbergen, A. Götz, J. Groeneveld, O. V. Gritsenko, M. Groening, S. Gusarov, F. E. Harris, P. van den Hoek, C. R. Jacob, H. Jacobsen, L. Jensen, J. W. Kaminski, G. van Kessel, F. Kootstra, A. Kovalenko, M. V. Krykunov, E. van Lenthe, D. A. McCormack, A. Michalak, M. Mitoraj, J. Neugebauer, V. P. Nicu, L. Noodleman, V. P. Osinga, S. Patchkovskii, P. H. T. Philipsen, D. Post, C. C. Pye, W. Ravenek, J. I. Rodríguez, P. Ros, P. R. T. Schipper, G. Schreckenbach, J. Seldenthuis, M. J. Seth, G. Snijders, M. Solá, M. Swart, D. Swerhone, G. te Velde, P. Vernooijs, L. Versluis, L. Visscher, O. Visser, F. Wang, T. A. Wesolowski, E. M. van Wezenbeek, G. Wiesenekker, S. K. Wolff, T. K. Woo and A. L. Yakovlev, *ADF2009, SCM, Theoretical Chemistry*, Vrije Universiteit, Amsterdam, The Netherlands, http://www.scm.com (accessed October 25, 2012).

18 S. El Ghachtouli, C. Cadiou, I. Déchamps-Olivier, F. Chuburu, M. Aplincourt and T. Roisnel, *Eur. J. Inorg. Chem.*, 2006, 3472.

19 Quantum yields of **L** and Zn : **L**$(NO_3)_2$ were investigated using quinine sulfate in a 0.5 mol L^{-1} H_2SO_4 solution as a reference (l_{exc} = 360 nm, l_{em} = 450 nm, ϕ = 0.55). Under these conditions f(**L**) = 0.4%, f(Zn : **L**$(NO_3)_2$) = 0.3%, and f(Zn_2 : **L**$(NO_3)_2$) = 2.6%; see Fig. S3 in the ESI.†

20 A. Gilbert and J. Baggott, *Essential of Molecular Photochemistry*, Blackwell, Oxford,U.K., 1991.

21 J. P. Perdew, K. M. Burke and M. Ernzerhof, *Phys. Rev. Lett.*, 1996, **77**, 3865.

22 S. Grimme, J. Anthony, S. Ehrlich and H. Krieg, *J. Chem. Phys.*, 2010, **132**, 154104.

23 O. V. Gritsenko, P. R. T. Schipper and E. J. Baerends, *Chem. Phys. Lett.*, 1999, **302**, 199; P. R. T. Schipper, O. V. Gritsenko, S. J. A. Van Gisbergen and E. J. Baerends, *J. Chem. Phys.*, 2000, **112**, 1344.

24 A. Klamt and G. G. Schürmann, *J. Chem. Soc., Perkin Trans. 2*, 1993, 799; A. Klamt and V. Jones, *J. Chem. Phys.*, 1996, **105**, 9972.

25 C. C. Pie and T. Ziegler, *Theor. Chem. Acc.*, 1999, **101**, 396.

26 E. Van Lenthe and E. J. Baerends, *J. Comput. Chem.*, 2003, **24**, 1142.

